EPJ Web of Conferences **258**, 10005 (2022) https://doi.org/10.1051/epjconf/202225810005
A Virtual Tribute to Quark Confinement and the Hadron Spectrum (vConf21)

Vortices in $\mathcal{PT}$ -symmetric non-Hermitian superfluid

Alexander Begun[1,*], *Maxim* Chernodub[1,2,], and *Alexander* Molochkov[1,]

[1]Pacific Quantum Center, Far Eastern Federal University, Sukhanova 8, Vladivostok 690950, Russia
[2]Institut Denis Poisson UMR 7013, Université de Tours, 37200 France

Abstract. We discuss the properties of the non-Hermitian $\mathcal{PT}$-symmetric two–scalar fields model. We investigate stability areas of this system and properties of vortices that emerge in the system of two interacting scalar fields. The phase diagram of the model contains stable and unstable regions depending on $\mathcal{PT}$-symmetry breaking, which intercross the regions of $U(1)$-symmetric and $U(1)$-broken phases in a nontrivial way. At non-zero quartic couplings, the non-Hermitian model possesses classical vortex solutions in the $\mathcal{PT}$-symmetric regions. We also consider a close Hermitian analog of the theory and compare the results with the non-Hermitian model.

1 Introduction

Traditional quantum mechanics requires the Hamiltonian to be Hermitian. This condition guarantees that the energy spectrum is real-valued and the time evolution of the system is unitary. However, as some studies show, the requirement of Hermiticity is optional rather than mandatory. The Hermiticity condition can be replaced by the requirement that the Hamiltonian of the system enjoys the invariance under the combined parity $\mathcal{P}$ and time-reversal inversion $\mathcal{T}$ operation ($\mathcal{PT}$-symmetry) [1, 2]:

$$H = H^{\mathcal{PT}}, \tag{1}$$

This symmetry of the Hamiltonian ensures the real-valued energy spectrum and, consequently, the unitary evolution and stability of the system unless the $\mathcal{PT}$-symmetry is broken spontaneously.

Examples of non-Hermitian Hamiltonians with real-valued energy spectrum appeared long ago in theoretical studies [3–5]. Nowadays, the ideas of non-Hermitian systems have found their applications in open systems with balanced gain and loss in different branches of physics, such as optics [6–11], photonics [12–16], superconducting wires [17, 18], $\mathcal{PT}$-symmetric electronic circuits [19] to mention a few.

In this work, we study vortex topological defects in a bosonic non-Hermitian model. We consider a model that consists of a pair of scalar fields associated with interacting condensates. The topological solutions in the multicomponent scalar models appear in various systems ranging from condensed matter to high energy physics. Some of these models can serve as viable extensions of the Standard Model of fundamental particle interactions [20–23].

*e-mail: begun.am@dvfu.ru

2 $\mathcal{PT}$-symmetric scalar field theory

We consider a simplest example of a scalar non-Hermitian $\mathcal{PT}$-symmetric theory which describes dynamics of two complex scalar fields ϕ_1 and ϕ_2 coupled by a mass matrix M. The Lagrangian of theory,

$$\mathcal{L} = \partial_\mu \Phi^\dagger \partial^\mu \Phi - \Phi^\dagger \hat{M}^2 \Phi - U_{int}(\Phi), \tag{2}$$

describes the doublet of two scalar fields $\Phi = \begin{pmatrix} \phi_1 \\ \phi_2 \end{pmatrix}$ subjected to the Hermitian self-interaction with the potential

$$U_{int}(\Phi) = \lambda|\phi_1|^4 + \lambda_2|\phi_2|^4 \,. \tag{3}$$

We consider a repulsive self-interaction with the quartic couplings $\lambda_{1,2} \geq 0$.

The non-Hermiticity emerges from the mass matrix of the Lagrangian (2), namely from the relative sign of its off-diagonal elements:

$$\hat{M}^2_{NH} = \begin{pmatrix} m_1^2 & m_5^2 \\ -m_5^2 & m_2^2 \end{pmatrix}. \tag{4}$$

The opposite signs in front of $m_5^2 \neq 0$ elements correspond to a non-Hermitian theory. The choice of the identical signs of off-diagonal elements (analytically) transforms the theory to its Hermitian counterpart with the mass matrix:

$$\hat{M}^2_{H} = \begin{pmatrix} m_1^2 & m_5^2 \\ m_5^2 & m_2^2 \end{pmatrix}. \tag{5}$$

To highlight the difference between these two types of theories, we rewrite their Lagrangians in terms of individual fields:

$$\begin{aligned} \mathcal{L}_{\rm NH} = \partial_\nu \phi_1^* \partial^\nu \phi_1 + \partial_\nu \phi_2^* \partial^\nu \phi_2 - m_1^2|\phi_1|^2 - m_2^2|\phi_2|^2 - m_5^2(\phi_1^*\phi_2 - \phi_2^*\phi_1) \\ -\lambda_1|\phi_1|^4 - \lambda_2|\phi_2|^4, \end{aligned} \tag{6}$$

$$\begin{aligned} \mathcal{L}_{\rm H} = \partial_\nu \phi_1^* \partial^\nu \phi_1 + \partial_\nu \phi_2^* \partial^\nu \phi_2 - m_1^2|\phi_1|^2 - m_2^2|\phi_2|^2 - m_5^2(\phi_1^*\phi_2 + \phi_2^*\phi_1) \\ -\lambda_1|\phi_1|^4 - \lambda_2|\phi_2|^4 \,. \end{aligned} \tag{7}$$

Both Hermitian and non-Hermitian models are invariant under the global U(1) transformation, in which the single phase factor (with a real-valued parameter ω) is shared by both complex scalar fields ϕ_1 and ϕ_2:

$$U(1): \qquad \Phi(t, \boldsymbol{x}) \to \Phi'(t, \boldsymbol{x}) = e^{i\omega}\Phi(t, \boldsymbol{x}) \tag{8}$$

The non-Hermitian theory (6) is also invariant under a discrete $\mathcal{PT}$ transformation that consists of the parity inversion $\mathcal{P}$ supplemented by the time conjugation $\mathcal{T}$:

$$\text{NH}: \quad \begin{cases} \mathcal{P}: & \Phi(t, \boldsymbol{x}) \to \Phi'(t, -\boldsymbol{x}) = \sigma_3\Phi(t, \boldsymbol{x}), \\ \mathcal{T}: & \Phi(t, \boldsymbol{x}) \to \Phi'(-t, \boldsymbol{x}) = \Phi^*(t, \boldsymbol{x}). \end{cases} \tag{9}$$

Notice that under the action of $\mathcal{P}$ transformation ϕ_1 transforms as a true scalar, while ϕ_2 transforms as a pseudo-scalar.

In the case of the Hermitian theory, the $\mathcal{P}$ and $\mathcal{T}$ transformations are as follows:

$$\text{H}: \quad \begin{cases} \mathcal{P}: & \Phi(t, \boldsymbol{x}) \to \Phi'(t, -\boldsymbol{x}) = \Phi(t, \boldsymbol{x}), \\ \mathcal{T}: & \Phi(t, \boldsymbol{x}) \to \Phi'(-t, \boldsymbol{x}) = \Phi^*(t, \boldsymbol{x}), \end{cases} \tag{10}$$

Notice that both fields ϕ_1 and ϕ_2 behave as true scalars under the parity inversion.

3 Ground states

In Ref. [24], an analytical study of the ground state of the two-field scalar model (2) has been done for a particular case when only one field was self-interacting ($\lambda_2 = 0$). We extend this analysis to the case of the most general model in which both scalar fields have nonzero self-interacting couplings, $\lambda_{1,2} \neq 0$. Unfortunately, such an extension makes the equations of motion much more complicated, which does not allow us to obtain analytical solutions. In our work, we use numerical analysis to find the ground state of the model as well as its $\mathcal{PT}$ stable regions.

The classical equations of motion can be obtained by the variation of the action corresponding to Lagrangian (6) with respect to the fields ϕ_1^* and ϕ_2^*, respectively:

$$\Box\phi_1 + m_1^2\phi_1 + m_5^2\phi_2 + \frac{\partial V}{\partial\phi_1^*} = 0\,, \tag{11}$$

$$\Box\phi_2 + m_2^2\phi_2 - m_5^2\phi_1 + \frac{\partial V}{\partial\phi_2^*} = 0\,. \tag{12}$$

In the ground state the condensates are coordinate-independent quantities, and Eqs. (12), can be reduced to the non-linear algebraic relations by representing fields ϕ_a in the radial form $\phi_a = v_a e^{i\theta_a}$:

$$m_1^2 v_1 + m_5^2 v_2 + 2\lambda_1 v_1^3 = 0\,, \tag{13a}$$

$$m_2^2 v_2 - m_5^2 v_1 + 2\lambda_2 v_2^3 = 0\,. \tag{13b}$$

In the case of the counterpart Hermitian model, the theory equations (13) take the following form:

$$m_1^2 v_1 + m_5^2 v_2 + 2\lambda_1 v_1^3 = 0\,, \tag{14a}$$

$$m_2^2 v_2 + m_5^2 v_1 + 2\lambda_2 v_2^3 = 0\,. \tag{14b}$$

These systems of equations can be solved numerically. Solutions that correspond to the minima of the energy density of the ground state

$$E_{\text{NH},0} = m_1^2 v_1^2 + m_2^2 v_2^2 + \lambda_1 v_1^4 + \lambda_2 \phi_2^4, \tag{15a}$$

$$E_{\text{H},0} = m_1^2 v_1^2 + m_2^2 v_2^2 + 2m_5^2 v_1 v_2 + \lambda_1 v_1^4 + \lambda_2 v_2^4, \tag{15b}$$

are represented in figure 1.

4 Stability of the ground state of non-Hermitian theory.

To probe the stability of the ground state, we consider weak fluctuations of the scalar fields,

$$\phi_a = v_a + \hat{\phi}_a, \tag{16}$$

with $|\hat{\phi}_a| \ll |v_a|$. Next, we build the quadratic fluctuation matrix that corresponds to the variation of action with respect to the small deviations of the fields about their ground-state values. The configuration is unstable if this matrix contains at least one negative eigenvalue.

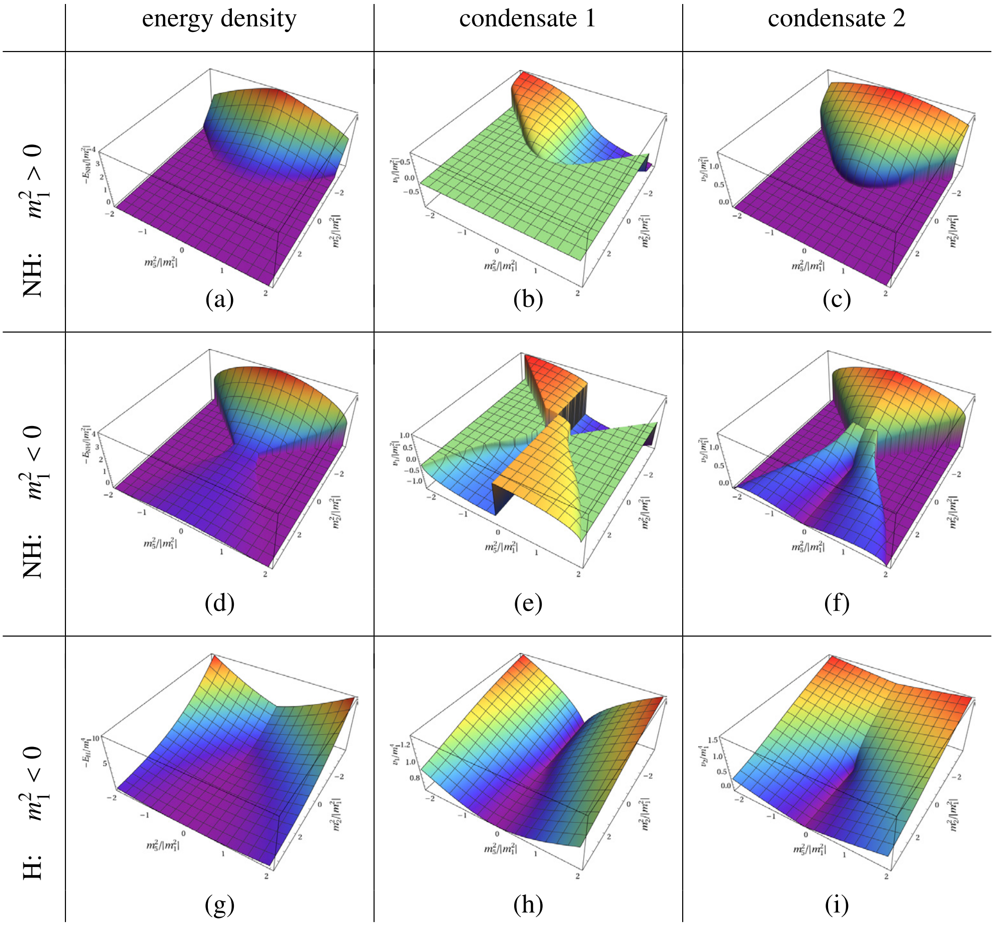

Figure 1. The upper panel depicts (a) the energy density and the condensates (b) v_1 and (c) v_2 in the ground state of the non-Hermitian model (6) with the real-valued mass of the field ϕ_1. The middle panel represents the same quantities obtained for the imaginary mass, $m_1^2 < 0$. The lower panel corresponds to the Hermitian theory (7). All quantities are shown in the units of the absolute value of the mass parameter, $|m_1|$. In all plots, the quartic couplings for both scalar fields are fixed: $\lambda_1 = \lambda_2 = 1$.

In the Hermitian theory, the minimum of energy of the system corresponds to the stable state as the quadratic fluctuation matrix does not contain negative eigenvalues. In the non-Hermitian theory, this criterion does not work in general and we are left with the additional analysis of its fluctuation matrix:

$$\mathcal{M}^2_{\rm NH} = \begin{pmatrix} 4\lambda_1 v_1^2 + m_1^2 & 2v_1^2\lambda_1 & m_5^2 & 0 \\ 2v_1^2\lambda_1 & 4\lambda_1 v_1^2 + m_1^2 & 0 & m_5^2 \\ -m_5^2 & 0 & 4\lambda_2 v_2^2 + m_2^2 & 2v_2^2\lambda_2 \\ 0 & -m_5^2 & 2v_2^2\lambda_2 & 4\lambda_2 v_2^2 + m_2^2 \end{pmatrix}. \tag{17}$$

In the U(1) broken phase, this matrix has one zero eigenvalue which corresponds to the Goldstone mode. In the symmetric U(1) phase, all eigenvalues are generally nonzero.

As it can be seen from figure 2, the ground state of the non-Hermitian model is unstable in some regions of the parameter space. We interpret these new regions as $\mathcal{PT}$-broken

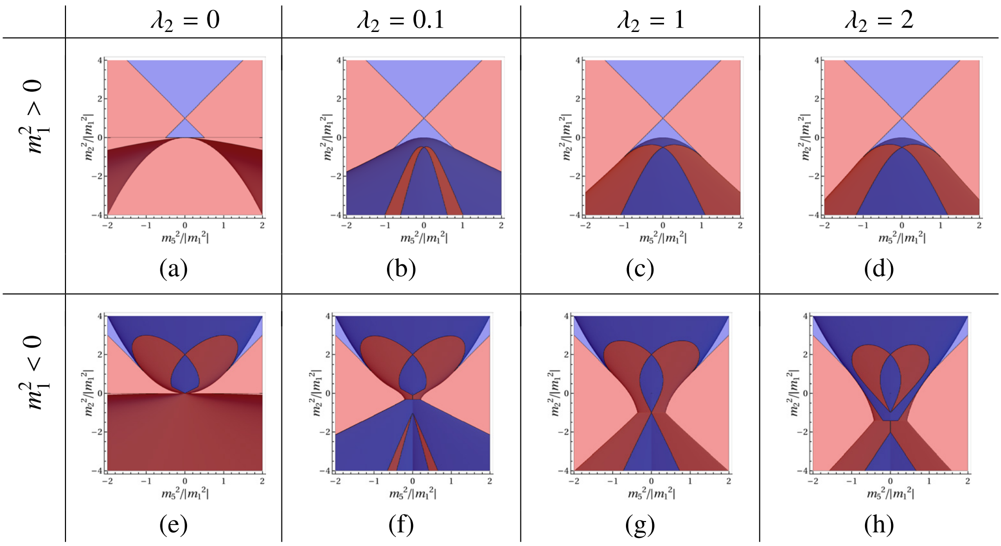

Figure 2. Stability diagrams of the non-Hermitian model in the (m_5^2, m_2^2) plane for the fixed coupling $\lambda_1 = 1$. The stable regions marked by the blue color and the unstable marked by the red color. The upper and panels correspond to $m_1^2 > 0$ and $m_1^2 < 0$, respectively. The dark (light) areas denote regions with non-vanishing (vanishing) condensates.

regions thus providing in our work the extension of the definition of the spontaneously $\mathcal{PT}$ breaking to the case of the interacting model. In the non-interacting limit, $\lambda_{1,2} \to 0$, the $\mathcal{PT}$-instability requirement reduces to the standard criterion of the $\mathcal{PT}$ breaking in the non-interacting model, $4m_5^4 > (m_1^2 - m_2^2)^2$. The system in the $\mathcal{PT}$-broken regions cannot be used as a valid prescription of any steady-state in a physical system. On the contrary, the $\mathcal{PT}$-symmetric regions are stable zones where the steady-state physics can be realized.

5 Vortices at finite couplings

Both Hermitian and non-Hermitian two-field models possess vortex solutions at finite values of the quartic couplings λ_1 and λ_2. We consider examples of the static vortex solutions of the classical equations of motion assuming the form of the scalar fields

$$\phi_a(r,\theta) = v_a f_a(r) e^{in\theta}\,, \qquad a = 1, 2,$$

where r and θ are the radial coordinates in the (x_1, x_2) plane and $n \in \mathbb{Z}$ is the vorticity of the solution.

The classical equations of motion are given by the following system of differential equations for the profile functions:

$$f_1''(r) + \frac{f_1'(r)}{r} - \frac{n^2}{r^2} f_1(r) - m_1^2 f_1(r) - m_5^2 \frac{v_2}{v_1} f_2(r) - 2\lambda_1 v_1^2 f_1^3 = 0, \tag{18}$$

$$f_2''(r) + \frac{f_2'(r)}{r} - \frac{n^2}{r^2} f_2(r) - m_2^2 f_2(r) + m_5^2 \frac{v_1}{v_2} f_1(r) - 2\lambda_2 v_2^2 f_2^3 = 0. \tag{19}$$

The equations on the profile functions in the counterpart Hermitian model are as follows:

$$f_1''(r) + \frac{f_1'(r)}{r} - \frac{n^2}{r^2} f_1(r) - m_1^2 f_1(r) + m_5^2 \frac{v_2}{v_1} f_2(r) - 2\lambda_1 v_1^2 f_1^3 \quad = \quad 0, \tag{20}$$

$$f_2''(r) + \frac{f_2'(r)}{r} - \frac{n^2}{r^2} f_2(r) - m_2^2 f_2(r) + m_5^2 \frac{v_1}{v_2} f_1(r) - 2\lambda_2 v_2^2 f_2^3 \quad = \quad 0. \tag{21}$$

Using the numerical analysis, we confirm the existence of the stable vortex solutions in the regions characterized by $U(1)$-broken symmetry and, simultaneously, obeying $\mathcal{PT}$-unbroken symmetry. In all other regions the stable vortex solutions do not exist.

An example of the profile functions for a set of coupling constants is shown in figure 3(a). The radial functions feature a linear rise close to the origin which turns into an exponentially slow approach to the corresponding vacuum expectation values at large distances. These properties mark the generic behaviour of all solutions that we have analyzed.

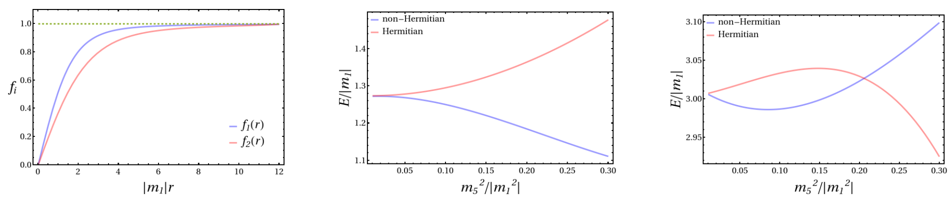

(a) (b) (c)

Figure 3. Panel (a) represents the profile functions of the elementary $n = 1$ vortex solution at the mass parameters $m_2^2 = |m_1^2|$ and $m_5^2 = 0.1|m_1^2|$ with $m_1^2 < 0$ and the equal quartic couplings $\lambda_1 = \lambda_2 = 1$. Panels (b) and (c) represent the Hermitian and non-Hermitian vortex energies respectively vs. the off-diagonal mass squared m_5^2 in different stability areas: (b) $m_2^2 = -m_1^2$ corresponds to the border of the stable and unstable regions and (c) $m_2^2 = 2.5m_1^2 < 0$ resides within the stable region of figure 2(g).

We show the vortex energies in both Hermitian and non-Hermitian theories in, respectively, in figure 3(b) and figure 3(c) in different areas of the phase diagram for the same values of the quartic couplings. While the vortex energies in the Hermitian and non-Hermitian versions trivially coincide with each other at $m_5 = 0$, their behaviour starts to differ from each other with the growth of the off-diagonal mass m_5.

6 Discussion and conclusion

Our work considers the non-Hermitian model of two self-interacting complex scalar fields. Due to the $\mathcal{PT}$-symmetry, this theory can describe open systems that exchange energy with an environment via gain and loss processes. It is the $\mathcal{PT}$-symmetry that provides an exact balance between the gains and losses, thus ensuring the stability of the ground state of the system.

The phase diagram of the non-Hermitian model and its comparison to the Hermitian counterpart are shown in figures 1 and 2, respectively. The Hermitian theory is stable in the whole parameter space. It has the U(1) broken phase with non-vanishing condensates everywhere except the line $m_5^2 = 0$. In contrast, the phase diagram of the non-Hermitian theory has complicated patterns (figure 2) enriched by the intersections of $\mathcal{PT}$-symmetric (stable) and $\mathcal{PT}$-broken (unstable) regions with U(1) symmetric and broken regions (with vanishing and non-vanishing condensates, respectively). This difference is caused by the nontrivial solutions of equations of motion in the case of $\mathcal{PT}$-symmetric self-interacting theory. The notion of the spontaneous $\mathcal{PT}$-breaking is generalized to the interacting model.

Similarly to the Hermitian theory, its non-Hermitian analog possesses the vortex solutions, stable only in the $\mathcal{PT}$-broken regions. We have investigated the vortex profiles and energies and found that the properties of single vortex solutions in the non-Hermitian case are qualitatively similar to the Hermitian ones, apart from the difference in the stability regions imposed by the $\mathcal{PT}$ symmetry in the non-Hermitian model.

Acknowledgement The work is supported by Grant No. 0657-2020-0015 of the Ministry of Science and Higher Education of Russia.

References

[1] C.M. Bender, S. Boettcher, Physical Review Letters **80**, 5243 (1998), `physics/9712001`
[2] C.M. Bender, Contemporary Physics **46**, 277 (2005), `quant-ph/0501052`
[3] E. Caliceti, S. Graffi, M. Maioli, Communications in Mathematical Physics **75**, 51 (1980)
[4] A.A. Andrianov, **140**, 82 (1982)
[5] T. Hollowood, Nuclear Physics B **384**, 523 (1992)
[6] S. Longhi, Physical Review Letters **105**, 013903 (2010)
[7] A. Guo, G.J. Salamo, D. Duchesne, R. Morandotti, M. Volatier-Ravat, V. Aimez, G.A. Siviloglou, D.N. Christodoulides, Physical Review Letters **103**, 093902 (2009)
[8] C.E. Rüter, K.G. Makris, R. El-Ganainy, D.N. Christodoulides, M. Segev, D. Kip, Optics and Photonics News **21**, 47 (2010)
[9] T. Kottos, Nature Physics **6**, 166 (2010)
[10] R. El-Ganainy, K.G. Makris, M. Khajavikhan, Z.H. Musslimani, S. Rotter, D.N. Christodoulides, Nature Physics **14**, 11 (2018)
[11] R. El-Ganainy, M. Khajavikhan, D.N. Christodoulides, S.K. Ozdemir, Communications Physics **2** (2019)
[12] L. Feng, R. El-Ganainy, L. Ge, Nature Photonics **11**, 752 (2017)
[13] R. El-Ganainy, K.G. Makris, D.N. Christodoulides, Z.H. Musslimani, Optics Letters **32**, 2632 (2007)
[14] K.G. Makris, R. El-Ganainy, D.N. Christodoulides, Z.H. Musslimani, Physical Review A **81**, 063807 (2010)
[15] K.G. Makris, R. El-Ganainy, D.N. Christodoulides, Z.H. Musslimani, International Journal of Theoretical Physics **50**, 1019 (2011)
[16] S. Longhi, Laser & Photonics Review **3**, 243 (2009)
[17] J. Rubinstein, P. Sternberg, Q. Ma, Physical Review Letters **99**, 167003 (2007)
[18] N.M. Chtchelkatchev, A.A. Golubov, T.I. Baturina, V.M. Vinokur, Physical Review Letters **109**, 150405 (2012)
[19] J. Schindler, A. Li, M.C. Zheng, F.M. Ellis, T. Kottos, Physical Review A **84**, 040101 (2011)
[20] J. Alexandre, J. Ellis, P. Millington, D. Seynaeve, Physical Review D **99**, 075024 (2019), `1808.00944`
[21] J. Alexandre, J. Ellis, P. Millington, D. Seynaeve, Physical Review D **98**, 045001 (2018), `1805.06380`
[22] A. Fring, T. Taira, Nuclear Physics B **950**, 114834 (2020), `1906.05738`
[23] J. Alexandre, J. Ellis, P. Millington, Physical Review D **102**, 125030 (2020), `2006.06656`
[24] P.D. Mannheim, Physical Review D **99**, 045006 (2019), `1808.00437`